

DOI: 10.15825/1995-1191-2020-4-89-97

FUNCTIONAL EFFICIENCY OF CELL-ENGINEERED LIVER CONSTRUCTS BASED ON TISSUE-SPECIFIC MATRIX (EXPERIMENTAL MODEL OF CHRONIC LIVER FAILURE)

M.Yu. Shagidulin^{1, 2}, N.A. Onishchenko¹, Yu.B. Basok¹, A.M. Grigoriev¹, A.D. Kirillova¹, E.A. Nemets¹, E.A. Volkova¹, I.M. Iljinsky¹, N.P. Mozheiko¹, V.I. Sevastianov¹, S.V. Gautier^{1, 2}

¹ Shumakov National Medical Research Center of Transplantology and Artificial Organs, Moscow, Russian Federation

² Sechenov University, Moscow, Russian Federation

Objective: to investigate the functional efficiency of a cell-engineered construct (CEC) of the liver based on tissue-specific matrix consisting of decellularized rat liver fragments, allogeneic liver cells and multipotent mesenchymal stromal cells (MSCs) isolated from the bone marrow on an experimental model of chronic liver failure (CLF). **Materials and methods.** In creating liver CECs, the liver for decellularization and liver cells were obtained from male Wistar rats. MSCs were isolated from rat bone marrow. The functional efficacy of CEC was investigated on an experimental CLF model obtained by priming rats with CCl₄ solution. At different periods after implantation, the outcomes were assessed based on the biochemical parameters of cytolysis. Morphological changes in the liver were analyzed by histochemical methods in the control (administration of saline solution into the liver parenchyma) and experimental (administration of liver CEC into the liver parenchyma) groups. **Results.** It was shown that implantation of the proposed CEC normalizes blood biochemical parameters and structural disorders of the damaged rat liver faster (by day 30 after introduction of CEC instead of day 180 in the control). The CEC was also shown to have reduced animal mortality from 50 to 0%, which is due to early activation of proliferation of viable liver cells and faster formation of new blood vessels. These effects are down to either stimulation of the internal regenerative potential of the damaged liver during CEC implantation or long-term functioning of the transplanted cells as part of the CEC based on the decellularized liver matrix. **Conclusion.** The liver CEC, implanted into the liver parenchyma in laboratory animals with a CLF model, has a functional activity.

Keywords: liver, liver failure, regeneration, cell-engineered constructs, bioartificial organs, matrixes.

INTRODUCTION

Liver transplantation is the gold standard treatment for end-stage liver disease. However, donor organ shortage limits the widespread use of this only radical method for treatment of decompensated cirrhosis. The number of patients requiring liver transplantation significantly exceeding the number of emerging organs suitable for transplantation indicates the need to develop alternative treatment options, among which the use of regenerative medicine and tissue engineering methods seems to be the most promising [1, 2].

Most of the technical approaches in the field of liver tissue engineering are based on isolation of primary hepatocytes or obtaining of hepatocyte-like cells from stem cells and 3D cultivation subsequently [3]. Note that it is advisable to use mesenchymal stromal cells in the composition of cell-engineered constructs (CECs) in the treatment of a number of liver diseases to stimulate organ regeneration [4]. Biocompatible and bioresorbable matrices are used to provide the CEC cells with favorable conditions for their vital activity.

In our opinion, decellularized carriers/scaffolds belonging to the class of biomimetics of the extracellular matrix (ECM) and obtained by removing cells and their fragments from tissue with maximum preservation of the structure and composition of natural ECM commands the greatest interest [5, 6].

A lot of work is devoted to whole organ decellularization by perfusion with surfactants and enzyme solutions [7]. A similar approach has been described for the heart, kidney, pancreas, and uterus [8–11]. Note that whole liver decellularization comes with several disadvantages: low efficiency in cell detritus removal and difficulty in penetration of cells, nutrients, and gases into the organ volume due to microcirculatory disorders. In previous works, we obtained a tissue-specific matrix from fragments of decellularized rat liver with intact structure and no cells and cell fragments [12]. The next logical step is to create liver CECs, consisting of a tissue-specific matrix, liver cells (LCs), and bone marrow-derived multipotent mesenchymal stromal cells (BM-MSCs) with subsequent proof of its functional efficiency in

an experimental model of chronic liver failure (CLF), which was the purpose of this work.

MATERIALS AND METHODS

To solve the set tasks, experimental studies were carried out on 60 male Wistar rats weighing 150–250 grams. The animals were kept in a vivarium at 18–20 °C temperature on a mixed diet with free access to water. Experiments on the animals were carried out from 9 to 19 hours at room temperature ($t = 22\text{--}24$ °C). All manipulations with the rats were carried out in accordance with the rules adopted by the European Convention for the Protection of Vertebrate Animals Used for Experimental and Other Scientific Purposes (ETS No. 123) Strasbourg, 1986).

The experiments were carried out on 60 male Wistar rats weighing 250 grams. Of these, 10 rats were used as LC donors and 10 rats as liver donors for decellularization. The experiment lasted for 180 days.

Rat liver fragments ($n = 10$) no larger than $2 \times 2 \times 2$ mm in size were obtained using a scalpel and scissors. Decellularization of rat liver fragments was carried out in three changes of phosphate-buffered saline (PBS) (138 mM NaCl, 2.67 mM KCl, 1.47 mM KH_2PO_4 , 8.1 mM Na_2HPO_4 , pH = 7.4) containing 0.1% sodium dodecyl sulfate and increasing Triton X-100 concentration: 1%, 2% and 3% [12]. The total decellularization time was 72 hours – 24 hours for each change of surfactants solution with magnetic stirrer. To obtain microparticles, decellularized liver fragments were placed in the CryoMill RETSCH cryomill (Retsch GmbH, Germany) and milled in a mode that included 3 milling cycles for 3 minutes at 25 Hz frequency. The fraction of 100–250 μm particles was separated using sieves of appropriate sizes.

Washing against surfactants included exposing the matrix to PBS containing an antibiotic (ampicillin, 20 $\mu\text{g}/\text{mL}$) and an antimycotic (amphotericin B, 2.0 $\mu\text{g}/\text{mL}$) for 96 hours. The washed samples were sterilized by γ -irradiation at 1.5 Mrad dose.

LCs and BM-MSCs were isolated and cultured in accordance with the general principles of carrying out culture studies on 10 male Wistar rats weighing 150 g.

To populate the decellularized liver matrix with cellular components according to a known technique [15], we used the previously established optimal cell ratio: LCs : BM-MSCs = 5 : 1 [17]. Prior to implantation, LCs and BM-MSCs were co-cultivated in the same 5 : 1 ratio for 3 days.

It should be noted that the introduction of BM-MSCs into the cellular component of CECs is due to their ability to induce cell proliferation processes, including through their own transdifferentiation [17].

The functional efficacy of the resulting liver CECs was evaluated in the CLF model.

CLF was modeled on male Wistar rats weighing 250 g ($n = 40$) by inoculating rats with CCl_4 solution according to our modified scheme [16]. Control of the adequacy

of the created CLF model was assessed by the level of mortality and survival of the animals, the state of blood biochemical parameters, and morphological characteristics of the liver state. At the CLF modeling stage, 9 rats (22.5%) died.

As a result, after CLF modeling, the surviving rats with the experimental CLF model were divided into 2 groups: control group 1 (16 animals) – saline was injected into the parenchyma of the damaged liver, and experimental group 2 (15 animals) – liver CECs were injected into the parenchyma of the damaged liver 7 days after CCl_4 injection. Immunosuppression was not used.

The rats from the control and experimental groups were taken out of the experiment on days 28–30, day 90 and day 180 by intraperitoneal administration of sodium thiopental in a dosage causing respiratory arrest. At the aforementioned periods, before complete respiratory arrest, venous blood was taken for biochemical studies. Liver function (ALT, ASAT, bilirubin, gamma-glutamyl transpeptidase (GGT), alkaline phosphatase levels) was studied using clinical chemistry analyser Reflotron™ (Roche, Switzerland) with special Reflotron™ test strips (measurement accuracy: $\pm 0.5\%$; reproducibility: $\leq 0.2\%$; linearity: $\pm 0.05\%$).

After complete respiratory arrest, the liver was explanted for morphological studies. We performed biopsies of healthy and damaged liver: liver failure without treatment – control; liver failure with treatment, studies were carried out in the CECs implantation areas and outside at days 28–30, day 90, and day 180 of the experiment. Data from light microscopy with staining of sections (H&E stain, Van Gieson and Mallory stains) were evaluated. We used a Leica DM 6000 B microscope and a Leica LTDCH 9435 camera (Germany).

Morphometric analysis was performed using the ImageScopeM software (Systems for Microscopy and Analysis, Russia) using a Leica DM 1000 microscope and a Leica LTDCH 9435 DFC 295 camera (Leica Camera AG, Germany). The presence of cirrhosis was determined morphometrically (counting the number of false lobules); specific area of connective tissue (%ratio to the total area of the liver section) [18, 19].

The viability of LCs in liver CECs was assessed using immunohistochemical staining with hepatocyte specific antigens (OCH1E5).

The results were statistically processed using statistical analysis software package BioStat. The significance of differences was assessed by Student's *t*-test, with the Bonferroni correction taken into account.

RESULTS AND DISCUSSION

After inoculation, the clinical condition of the surviving animals was characterized by decreased body weight, adynamia and partial baldness. After inoculation, during the entire experiment (180 days), 50% ($n = 8$) more rats in the control group died against the background of CLF at different times. In the experimental

group, the survival rate by the same period was 100%. In this regard, assessment of functional and morphological changes in the liver of the experimental rats after CLF modeling was studied in 8 and 15 rats in the control and experimental groups, respectively. Absence of mortality in the experimental group allowed us to conclude that the implanted CECs had a positive effect on the survival rate of the CLF model rats. Fig. 1 shows a macropreparation of rat liver after the end of inoculation, i.e. day 42 from the start of CCl_4 inoculation. The liver was dense and enlarged. The surface was shallowly, finely grained, with rounded edges.

Microscopically, within the first month after the end of inoculation, a typical picture of cirrhotic transformation of the liver architectonics with progressive disorder in its structure at later follow-up periods (especially at days 60 and 90) due to connective tissue proliferation and emerging fibrosis was revealed (Fig. 2).

After decellularization [12], liver fragments were washed completely of LCs (Fig. 3), followed by colonization of the resulting tissue-specific matrix with cellular components of LCs and BM-MSCs.

The histological data presented in Fig. 4 demonstrate the presence of adherent hepatocytes on the decellularized matrix of rat liver.

At day 90 and 180 after implantation of CECs, representing finely dispersed particles of decellularized liver tissue with LCs and BM-MSCs seeded on it in a 5 : 1 ratio, viable and functioning hepatocytes were detected (Fig. 5).

At day 90, donor liver cells co-cultured with BM-MSCs formed associates of viable and functionally active cells within CECs. There were no pronounced inflammatory reactions and signs of rejection. Similar data were obtained at day 180 of CECs implantation.

To quantify the changes occurring in the liver structure of the CLF model rats in both groups, a morpho-



Fig. 1. Rat liver after injection, 42 days

metric study of the state of non-parenchymal structures (determination of the specific area of connective tissue and the number of false lobules in the liver) was carried out at different times for 180 days. It was found that in group 2, 60–90 days after administration of CECs, restoration of both parenchyma and non-parenchymal

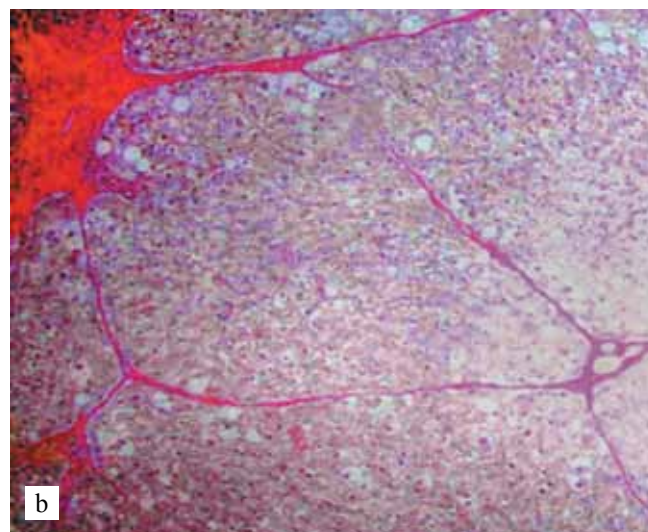
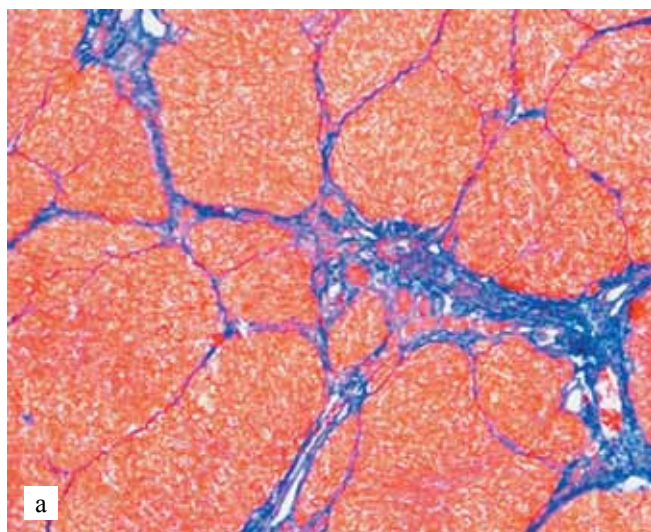


Fig. 2. Rat liver tissue after CLF modeling (CCl_4 injection = 42 days). a) 90 days, false lobules. Mallory staining for connective tissue. Microscope magnification 100 \times . b) 180 days, formed false lobules, sclerosis and cirrhosis. Van Gieson's stain. 100 \times

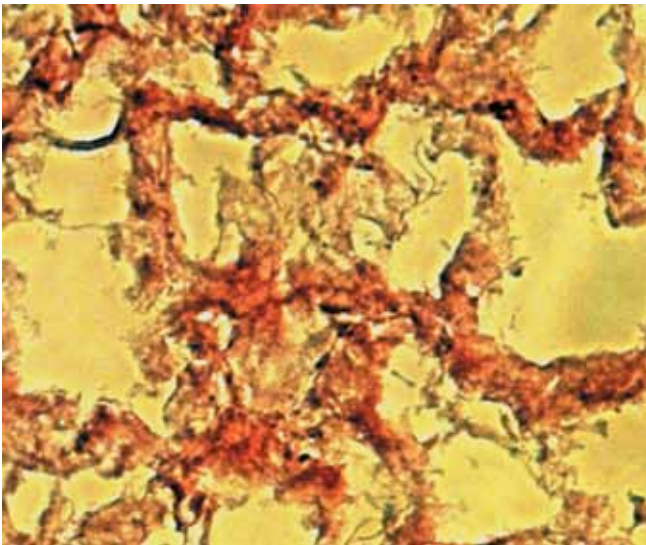


Fig. 3. Fragment of decellularized rat liver. H&E stain. 200×

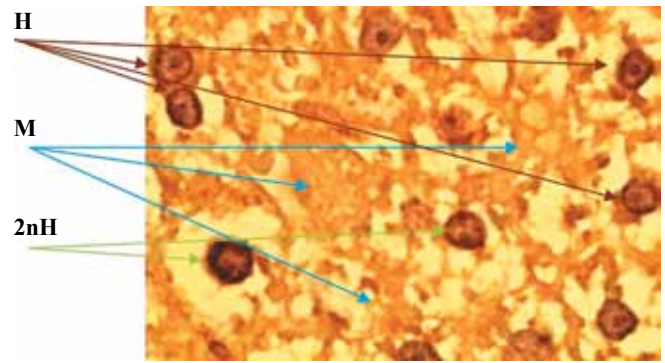


Fig. 4. Hepatocytes adhered to the tissue-specific liver matrix: M – decellularized liver matrix; H – adhered hepatocytes; 2nH – binuclear hepatocytes. H&E stain. 400×

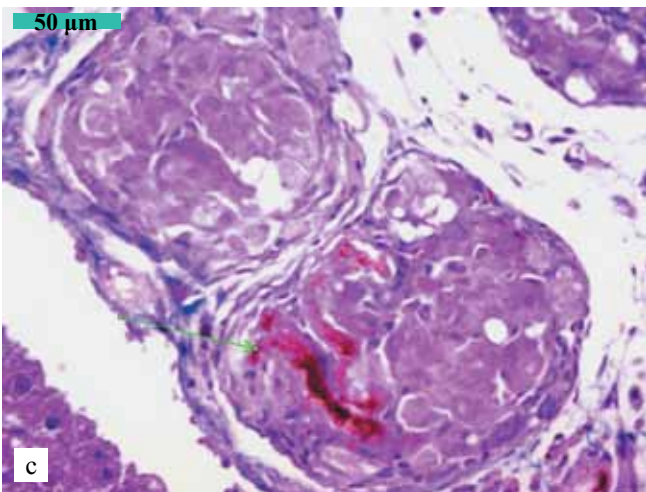
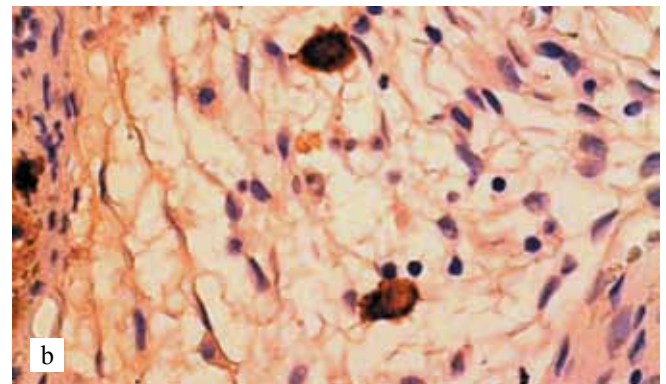
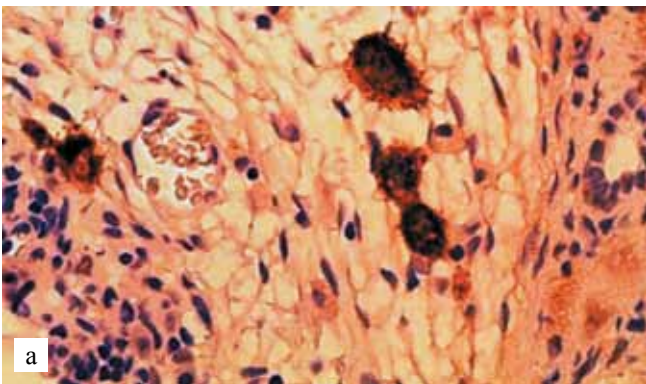


Fig. 5. Histological liver preparations in the CEC transplanted area (LC : MMSC BM = 5 : 1) in the parenchyma of the damaged liver: viable hepatocytes at 90 (a) and 180 (b) days. Immunohistochemical study with hepatocyte-specific antigens (OCH1E5) – positive granular cytoplasmic staining; c – Bile production (green arrow) by transplanted hepatocytes. H&E stain, 400×

structures occurred. This is confirmed by a dynamic morphometric study of the decrease in the specific area of the liver connective tissue and the number of false lobules in it (Fig. 6).

Liver function was assessed over time by measuring the serum biochemical parameters. Determination of the level of cytolysis enzymes (ALT, ASAT, ALP) in the blood serum of the rats (Fig. 7) made it possible to establish a sharp increase in the level of these enzymes

during the first 2 weeks of inoculation. After the end of the inoculation, 7 days later, ALT and AST levels increased by more than 4.5 and 3 times, respectively, while ALP levels increased by almost 5 times. 28–30 days after the end of the inoculation, the levels of cytolysis enzymes decreased, but continued to remain at a significantly ($p < 0.05$) higher level for a long time (Fig. 7) for 180 days compared with normal values in intact animals. In the experimental group, cytolitic processes were also

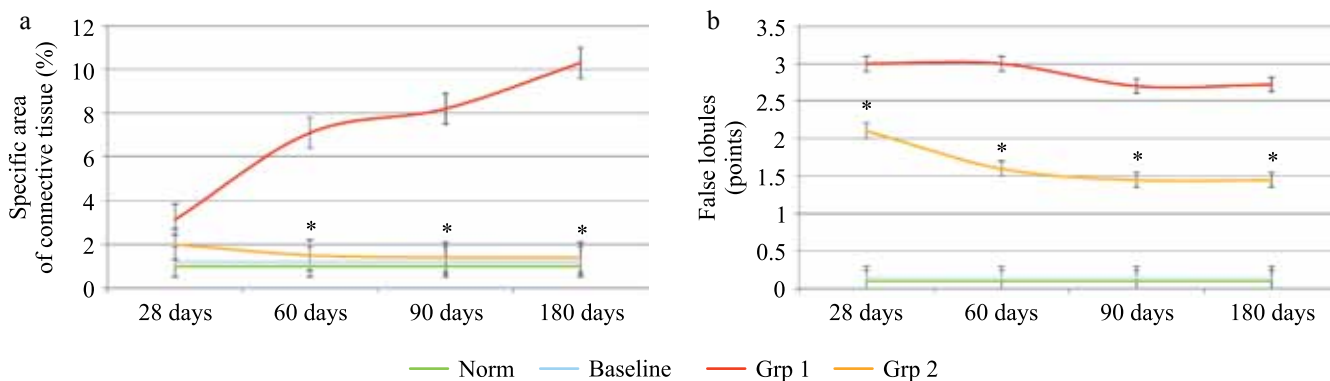


Fig. 6. Dynamic morphometric assessment of the state of non-parenchymal structures of the rat liver during CLF modeling and CEC implantation. a – change in the specific area of connective tissue; b – counting the number of false lobules in the liver: group 1 – control (saline); group 2 – liver CEC. * The difference is significant compared to the level of the indicator in the rat liver in the control group, $p < 0.05$

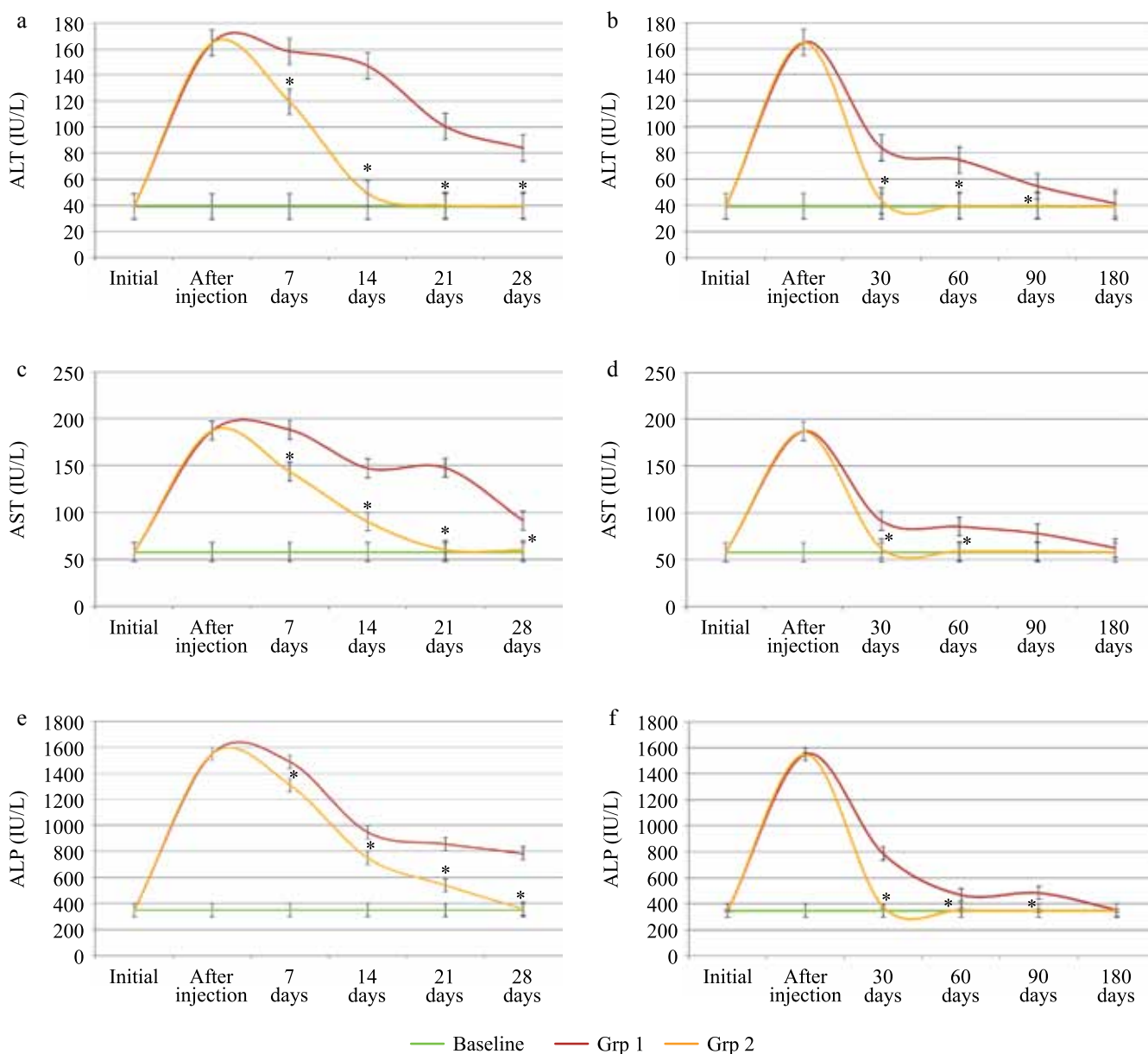


Fig. 7. Dynamics of normalization of the cytolysis enzymes level (ALT, AST, ALP) in the blood serum of rats after CLF modeling and CEC implantation. Level for healthy rats: ALT up to 40 IU/L; AST – up to 60 IU/L; ALP – up to 350 IU/L. a, b, e – observation period 28 days; b, d, f – observation period 180 days. * The difference is significant compared to the level of enzymes in the control (group 1); $p < 0.05$

observed in the liver parenchymal cells, but which were significantly less intense than in the control group. The corresponding indicators reached normal values by 30 days after CECs implantation, while for the control, the AST, ALT, and ALP levels normalized only at day 180 of the experiment (Fig. 7).

The serum gamma-glutamyl transpeptidase (γ -GTP) and bilirubin levels in the experimental animals remained within the normal range at all follow-up periods.

The observed effects could be due to stimulation of the intrinsic regenerative potential of the damaged liver during CECs implantation, or by the active functioning of the transplanted cells within CECs based on the decellularized liver matrix.

CONCLUSION

Implantation of the proposed CECs provides a more rapid normalization of biochemical blood parameters and structural disorders in the damaged rat liver (at day 30 after introduction of CECs instead of day 180 as was obtained in the control) and reduced animal mortality from 50% to 0% due to earlier activation of viable LCs proliferation processes and faster formation of new blood vessels.

Thus, the outcomes obtained prove that liver CECs implanted into the liver parenchyma of laboratory CLF model animals have a functional activity.

The authors declare no conflict of interest.

REFERENCES

1. *Salim MS, Issa AM, Farrag ARH, Gabr H.* Decellularized liver bioscaffold: a histological and immunohistochemical comparison between normal, fibrotic and hepatocellular carcinoma. *Clin Exp Hepatol.* 2019; 5 (1): 35–47. doi: 10.5114/ceh.2019.83155.
2. *Acun A, Oganessian R, Uygun BE.* Liver bioengineering: promise, pitfalls, and hurdles to overcome. *Curr Transplant Rep.* 2019; 6 (2): 119–126. doi: 10.1007/s40472-019-00236-3.
3. *Mazza G, Al-Akkad W, Rombouts K, Pinzani M.* Liver tissue engineering: from implantable tissue to whole organ engineering. *Hepatol Commun.* 2017; 2 (2): 131–141. doi: 10.1002/hep4.1136.
4. *Elchaninov A, Fatkhudinov T, Usman N, Arutyunyan I, Makarov A, Lokhonina A et al.* Multipotent stromal cells stimulate liver regeneration by influencing the macrophage polarization in rat. *World J Hepatol.* 2018; 10 (2): 287–296. doi: 10.4254/wjh.v10.i2.287.
5. *Crapo PM, Gilbert TW, Badylak SF.* An overview of tissue and whole organ decellularization processes. *Biomaterials.* 2011; 32 (12): 3233–3243. doi: 10.1016/j.biomaterials.2011.01.057.
6. *Uygun BE, Yarmush ML, Uygun K.* Application of whole-organ tissue engineering in hepatology. *Nature Reviews Gastroenterology & Hepatology.* 2012; 9 (12): 738–744. doi: 10.1038/nrgastro.2012.140.
7. *Rossi EA, Quintanilha LF, Nonaka CKV, Souza BSF.* Advances in hepatic tissue bioengineering with decellularized liver bioscaffold. *Stem Cells Int.* 2019; 2019: 2693189. doi: 10.1155/2019/2693189.
8. *Ferng AS, Connell AM, Marsh KM, Qu N, Medina AO, Bajaj N et al.* Acellular porcine heart matrices: whole organ decellularization with 3D-bioscaffold & vascular preservation. *J Clin Transl Res.* 2017; 3 (2): 260–270.
9. *Figliuzzi M, Bonandrini B, Remuzzi A.* Decellularized kidney matrix as functional material for whole organ tissue engineering. *J Appl Biomater Funct Mater.* 2017; 15 (4): e326–e333. doi: 10.5301/jabfm.5000393.
10. *Kuna VK, Kvarnström N, Elebring E, Holgersson SS.* Isolation and decellularization of a whole porcine pancreas. *J Vis Exp.* 2018; (140): 58302. doi: 10.3791/58302. PMID: 30371658.
11. *Daryabari SS, Kajbafzadeh AM, Fendereski K, Ghorbani F, Dehnavi M, Rostami M et al.* Development of an efficient perfusion-based protocol for whole-organ decellularization of the ovine uterus as a human-sized model and in vivo application of the bioscaffolds. *J Assist Reprod Genet.* 2019; 36 (6): 1211–1223. doi: 10.1007/s10815-019-01463-4.
12. *Gautier SV, Sevastyanov VI, Shagidulin MYu, Nemets EA, Basok YuB.* Tkanespetsificheskiy matriks dlya tkanevoy inzhenerii parenkhimatoznogo organa i sposob ego polucheniya. Patent na izobretenie RU 2693432 C2, 02.07.2019.
13. *Shumakov VI, Onishhenko NA.* Biologicheskie rezervy kletok kostnogo mozga i korekcija organnyh disfunkcij: [monografija]. M.: Lavr, 2009. 307.
14. *Gautier SV, Shagidulin MYu, Onishhenko NA, Krascheninnikov ME, Nikol'skaja AO, Bashkina LV, Sevast'janov VI.* Sposob lechenija pechenochnoj nedostatochnosti. Patent na izobretenie RU 2586952 C1, 10.06.2016.
15. *Shagidulin MYu, Onishchenko NA, Krascheninnikov ME, Iljinsky IM, Mogeiko NP, Shmerko NP et al.* Survival of liver cells, immobilized on 3d-matrixes, in liver failure model. *Russian Journal of Transplantology and Artificial Organs.* 2011; 13 (3): 59–66. [In Russ, English abstract]. doi: 10.15825/1995-1191-2011-3-59-66.
16. *Nicol'skaja AO, Gonikova ZZ, Kirsanova LA, Shagidulin MJu, Onishhenko NA, Sevast'janov VI.* Sposob modelirovaniya tjazhjologo spontanno neobratimogo povrezhdenija pecheni. Patent na izobretenie RU 2633296 C, 11.10.2017.
17. *Shagidulin MYu, Onishchenko NA, Krascheninnikov ME, Nikol'skaja AO, Volkova EA, Il'inskij IM et al.* The influence of the ratio of liver cells and bone marrow in the implantable cell-engineering structures of the liver on the recovery efficiency of functional and morphological parameters in chronic liver failure. *Russian Journal of Transplantology and Artificial Organs.* 2019; 21 (1): 122–134. [In Russ, English abstract]. doi: 10.15825/1995-1191-2019-1-122-134.
18. *Avtandilov GG.* Medicinskaja morfometrija. Rukovodstvo. M.: Medicina, 1990. 384.
19. *Ishak K., Baptista A, Bianchi L, Callea F, Grootes J et al.* Gistologicheskaya ocenka stadii i stepeni hronicheskogo gepatita. *Klinicheskaya gepatologiya.* 2010; 2: 8–11.

The article was submitted to the journal on 14.10.2020